Journal of Organometallic Chemistry 875 (2018) 80–87

Contents lists available at ScienceDirect

Journal of Organometallic Chemistry

journal homepage: www.elsevier.com/locate/jorganchem

Synthesis, structure, and reactivity of doubly *trans*-spanning bis(dialkyl selenide) complexes; a new route to diselenamacrocycles via alkene metathesis in metal coordination spheres

Hemant Joshi, Sugam Kharel, Nattamai Bhuvanesh, John A. Gladysz*

Department of Chemistry, Texas A&M University, PO Box 30012, College Station, TX, 77842-3012, USA

ARTICLE INFO

Article history:
Received 4 August 2018
Received in revised form
25 August 2018
Accepted 29 August 2018
Available online 31 August 2018

"To our colleague Richard Puddephatt in appreciation of his many contributions to the organometallic chemistry of the noble metals"

Keywords:
Platinum
Selenium
Grubbs' first generation catalyst
Alkene metathesis
Hydrogenation
Crystal structures

ABSTRACT

The reaction of selenium with $NaBH_4$ and $Br(CH_2)_6CH{=}CH_2$ (2.0 equiv each) gives the dialkyl selenide $Se((CH_2)_6CH{=}CH_2)_2$ (91% after workup) which is combined with $PtCl_2$ (0.5 equiv, toluene) to give *trans*-$PtCl_2(Se((CH_2)_6CH{=}CH_2)_2)_2$ (**10**, 85%). The reaction of **10** and Grubbs' first generation catalyst yields macrocyclic *trans*-$PtCl_2(Se((CH_2)_6CH{=}CH(CH_2)_6)_2Se)$ (**11**, 60%) as a mixture of *syn*/*anti* isomers with respect to the selenium lone pairs. The reaction of **11** and Ph_2Zn gives the diphenyl complex *trans*-$PtPh_2(Se((CH_2)_6CH{=}CH(CH_2)_6)_2Se)$ (**12**, 86%; mixture of isomers). When **11** is treated with H_2 under conditions that hydrogenate related diphosphine complexes (5 bar, 50 °C, $(Ph_3P)_3RhCl$ or PtO_2, CH_2Cl_2), no reaction occurs. Under more forcing conditions, (8 bar, 85 °C, Pd/C, C_2H_5OH), **11** and **12** give the demetalated diselenamacrocycle $Se(C_{14}H_{28})_2Se$ (**13**; 72-67%). The crystal structures of **11** and **12** show *anti* selenium lone pairs and *trans* C=C linkages; that of **13** exhibits columns of extended macrocycles.

1. Introduction

Metal complexes with sterically restricted coordination spheres offer unique domains for catalysis that potentially lead to new activities and selectivities [1]. For some time, we have sought to engineer such environments via three fold intramolecular ring closing metatheses of metal complexes with triply olefinic *trans* ligands of the formula $E((CH_2)_mCH{=}CH_2)_3$ (E = P, As; $m = 4–14$) [2–5], as exemplified in Scheme 1. The crude products, which are usually mixtures of *cis*/*trans* C=C isomers, are then hydrogenated to give cage like complexes with three methylene chains linking the *trans* disposed heteroatoms. These assemblies are also of interest in the context of molecular rotors and gyroscopes [6].

For various reasons, we have also prepared similar adducts from complexes with doubly olefinic *trans* phosphine ligands $PhP((CH_2)_mCH{=}CH_2)_2$ [7–9]. As shown in Scheme 2, these feature two methylene chains, and can exhibit two stereoisomers that differ in the *syn*/*anti* disposition of the unique phosphorus substituent (Ph). In the case of the platinum pentafluorophenyl chloride complex **6c**, both forms have been isolated and crystallographically characterized [7]. We sought to expand these doubly *trans* spanning systems to a wider range of donor atoms, especially those that might be further functionalized, such as via a lone pair [10]. Accordingly, we initiated a feasibility study with doubly olefinic selenium donor ligands, the successful results of which are reported herein, together with structural and reactivity data.

2. Results

Selenium powder was treated with the hydride reagent $NaBH_4$ (2.0 equiv) to generate a functional equivalent of Na_2Se [11]. The subsequent addition of $Br(CH_2)_6CH{=}CH_2$ (2.0 equiv) afforded the doubly olefinic dialkyl selenide $Se((CH_2)_6H{=}CH_2)_2$ (**9**) as a light yellow oil in 91% yield after workup. Compound **9**, and all other new species below, were characterized by NMR (1H, $^{13}C\{1H\}$) and

* Corresponding author.
E-mail address: gladysz@mail.chem.tamu.edu (J.A. Gladysz).

https://doi.org/10.1016/j.jorganchem.2018.08.029
0022-328X/

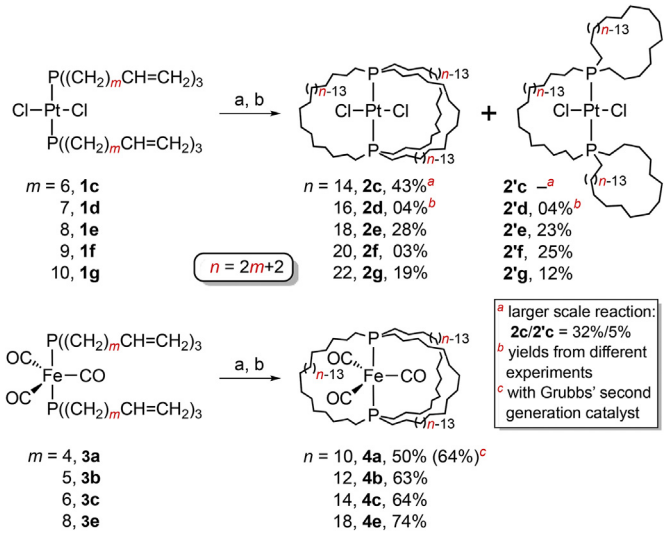

Scheme 1. Representative complexes in which three methylene chains link *trans* disposed phosphorus atoms: (a) Grubbs' first generation catalyst; (b) H_2/catalyst.

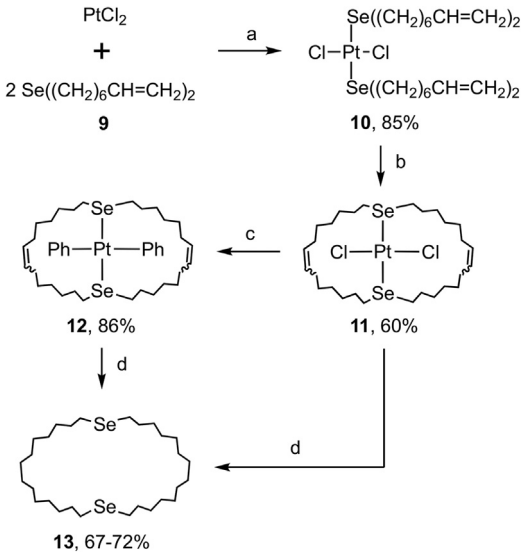

Scheme 3. Syntheses of new selenium containing compounds: (a) toluene; (b) Grubbs' first generation catalyst, refluxing CH_2Cl_2; (c) Ph_2Zn, THF; (d) Pd/C, 8 bar H_2, 85 °C.

IR spectroscopy, as well as microanalysis. As summarized in the experimental section, all features were routine.

As shown in Scheme 3, $PtCl_2$ and **9** (2.0 equiv) were combined in toluene. After 48 h, workup gave the expected product *trans*-$PtCl_2(Se((CH_2)_6CH{=}CH_2)_2)_2$ (**10**) as an air stable yellow oil in 85% yield. None of the NMR or IR data rigorously distinguished between *trans* and *cis* geometries. However, *trans*-PtX_2L_2 species, which lack permanent dipole moments, are more commonly isolated from reactions in nonpolar solvents [3,12]. Also, all of the crystal structures of complexes derived from **10** exhibit *trans* geometries (*vide infra*).

Next, a 0.0027 M CH_2Cl_2 solution of **10** was treated with Grubbs' first generation catalyst (3.1 mol%). The mixture was refluxed (48 h) and then chromatographed to give macrocyclic *trans*-$PtCl_2(Se((CH_2)_6CH{=}CH(CH_2)_6)_2Se)$ (**11**) in 60% yield as a light yellow solid that melted without decomposition at 116 °C. The $^{13}C\{^1H\}$ NMR spectrum (CD_2Cl_2) showed a mixture of two dominant isomers. No decoalescence phenomena or new signals were observed when spectra were recorded at −90 °C.

Additional $^{13}C\{^1H\}$ NMR spectra were recorded in C_6D_5Br at elevated temperatures. As shown in the supporting information (Figure s1), most signals coalesced (361–393 K), indicating interconversion of the isomers. Such facile equilibration would not be expected for *Z*/*E* C=C linkages. Importantly, there have been detailed studies of pyramidal inversions of dialkyl selenide ligands in *trans*-$PtCl_2(SeEt_2)_2$ and the corresponding dibromide, diiodide, and palladium complexes [13]. NMR signals were observed to coalesce at 301–363 K (60 MHz instrument), corresponding to barriers of 15.6–18.2 kcal/mol. Thus, the isomers of **11** were presumed to differ in the *syn*/*anti* orientation of the selenium lone pairs, akin to the two forms of *trans*-**6c** in Scheme 2. The C=C moieties were presumed to be *trans* (or predominantly so), as inferred from two crystal structures below.

The corresponding complexes of $PtCl_2$ and the dibridgehead diphosphines $P((CH_2)_n)_3P$ ($n = 14, 18$), *trans*-**2c,e** (Scheme 1), readily react with Ph_2Zn to give the analogous diphenyl complexes [3a,14]. Thus, **11** and Ph_2Zn (3.0 equiv) were combined in THF. Workup gave the target complex *trans*-$PtPh_2(Se((CH_2)_6CH{=}CH(CH_2)_6)_2Se)$ (**12**) in 86% yield as a white powder, again as a mixture of presumably *syn*/*anti* isomers.

Next, hydrogenation conditions analogous to those used in Schemes 1 and 2 were applied to **11**. However, reactions in CH_2Cl_2 at 50 °C under 5 bar of H_2 and with either PtO_2 or $(Ph_3P)_3RhCl$ as catalysts (20 mol%) gave, after 96 h, no detectable conversion. Reactions of **11** and **12** were then conducted in C_2H_5OH at 85 °C under 8 bar of H_2 with 10% Pd/C (50 mol%). In both cases, workups gave the same white solid in 67–72% yields, which as established below proved to be the demetalated hydrogenated diselenamacrocycle $Se(C_{14}H_{28})_2Se$ (**13**).

Compounds **11**–**13** could be crystallized as described in the experimental section. The structures were solved as outlined in Table 1 and the experimental section. Two independent molecules of **11** were present in the unit cell. These differed primarily in the conformations or *gauche*/*anti* sequences of the macrocycles. Some short methylene segments of **12** were disordered, but this could be modeled (50:50 occupancy over two positions). Key interatomic distances and angles are given in Table 2, and the molecular structures are depicted in Figs. 1–3. All of the individual molecules

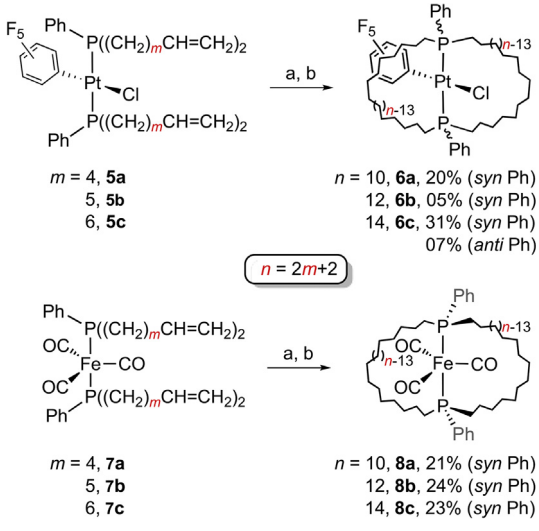

Scheme 2. Representative complexes in which two methylene chains link *trans* disposed phosphorus atoms: (a) Grubbs' first generation catalyst; (b) H_2/catalyst.

featured an inversion center, as reflected by the atom labels. As foreshadowed above, both **11** and **12** were *trans*, *trans* C=C isomers. Additional structural features are analyzed in the discussion section.

3. Discussion

This study establishes that the chemistry in Scheme 2 is easily extended to related dialkyl selenide complexes. The C=C metatheses are not adversely effected by the presence of selenium, which has a stereochemically and potentially chemically active lone pair. As shown in Scheme 4, this is in line with earlier results with the doubly olefinic *cis* platinum bis(dialkyl sulfide) complexes **14** [15]. However, the hydrogenations in Scheme 3 are adversely affected by the presence of selenium, although perhaps with further experimentation a procedure that does not detach the macrocycle from platinum might be found. No hydrogenations of the bis(dialkyl sulfide) complex **15** (which could potentially turn out similarly) were attempted.

The *anti* and *syn* isomers of **11** and **12** can be represented schematically as in **I** and **II** in Scheme 5 (top). In the former, C_a and C_c, and C_b and C_d, are homotopic (exchanged by a C_2 symmetry axis); in the latter C_a and C_d, and C_b and C_c, are homotopic. As shown, a single pyramidal inversion at selenium is sufficient to exchange all selenium bound carbon atoms (and other carbon atoms in the macrocycle). In other dynamic processes involving dialkyl sulfide and selenide ligands, both inversion and metal/donor atom bond rotation must take place to consummate exchange [13,16].

Figs. 1 and 2 show that **11** and **12** crystallize as *anti* isomers (**I**). Although lone pairs are not represented in thermal ellipsoid plots, the *anti* dispositions of the C–Se–C linkages are evident when the Se–Pt–Se axes are perpendicular to the plane of the paper. Given the crystal structures, and the ready interconversion of *syn* and *anti* isomers, we provisionally assign the latter as more stable. However, *syn* isomers always dominate with the related platinum

Table 2
Key crystallographic distances [Å] and angles [°].[a]

	11[b]	**11**[b]	**12**
Pt–Se	2.4186(4)	2.4243(4)	2.3929(6)
	2.4186(4)	2.4243(4)	2.3929(6)
Pt-X[c]	2.3026(9)	2.2981(9)	2.076(5)
	2.3026(9)	2.2981(9)	2.076(5)
Se–Se	4.8371(8)	4.8486(8)	4.7558(11)
Se–C	1.955(4)	1.959(4)	1.956(5)
	1.961(4)	1.967(4)	1.945(6)
Se–Pt–Se	180.00(0)	180.00(0)	180.00(2)
Se–Pt–Cl	84.97(3)	87.20(3)	85.90(13)
	84.97(3)	87.20(3)	85.90(13)
	95.03(3)	92.80(3)	94.10(13)
	95.03(3)	92.80(3)	94.10(13)
X-Pt-X	180.00(0)	180.00(0)	180.00(0)
C–Se–C	100.37(17)	105.85(11)	100.10(2)
C–Se–Pt	109.51(12)	105.85(11	104.36(15)
	104.19(12)	101.12(12)	102.99(18)
LP-Se–C	100.37(17)	105.85(11)	100.10(2)
LP-Se–Se-LP	180.00	180.00	180.00
C–Se–Se–C	180.00	180.00	180.00
	73.35	77.58	75.83

[a] The numerous degeneracies are a result of the inversion centers (see text).
[b] Values for the two independent molecules in the unit cell.
[c] Distances from platinum to the ligating atoms of the non-phosphine ligands.

Table 1
Summary of crystallographic data.

	11	**12**	**13**
empirical formula	$C_{28}H_{52}Cl_2PtSe_2$	$C_{40}H_{62}PtSe_2$	$C_{28}H_{56}Se_2$
formula weight	812.60	895.90	550.64
temperature [K]	99.88	110.15	100.0
diffractometer	Bruker Venture	Bruker Apex 2	Bruker Venture
wavelength [Å]	1.54178	0.71073	1.54178
crystal system	Triclinic	Monoclinic	Monoclinic
space group	*P*-1	C_12/c_1	P_12_1/c_1
unit cell dimensions:			
a[Å]	10.1740(5)	9.7643(15)	5.4228(2)
b[Å]	10.5714(5)	14.337(2)	34.7343(11)
c[Å]	14.6487(7)	27.693(4)	7.9073(3)
α[°]	86.217(2)	90	90
β[°]	88.611(2)	93.490(2)	107.515(2)
γ[°]	89.310(2)	90	90
V[Å^3]	1571.54(13)	3869.4(10)	1420.35(9)
Z	2	4	2
ρ_{calc}[Mg/m^3]	1.717	1.538	1.288
μ[mm^{-1}]	12.654	5.532	3.317
F(000)	800	1792	584
crystal size [mm^3]	0.34 × 0.21 × 0.03	0.42 × 0.26 × 0.24	0.26 × 0.12 × 0.018
θ limit[°]	4.191 to 70.654	2.527 to 28.195	2.544 to 70.017
index range (*h*, *k*, *l*)	−12, 12, −12, 12, −17, 17	−12, 12, −18, 18, −36, 36	−6, 6; −42, 42; −9, 9
reflections collected	44553	48342	17649
independent reflections	5942	4745	2701
R(int)	0.0408	0.0375	0.0620
completeness to θ	99.4	100.0	99.8
max. and min. transmission	0.8295 and 0.1015	0.7457 and 0.4258	0.4684 and 0.3482
data/restraints/parameters	5942/0/301	4745/161/277	2701/0/136
goodness-of-fit on F^2	1.041	1.476	1.222
R indices (final) [$I > 2\sigma(I)$]			
R_1	0.0259	0.0379	0.0461
wR_1	0.0609	0.0814	0.0859
R indices (all data)			
R_2	0.0291	0.0400	0.0575
wR_2	0.0624	0.0820	0.0896
largest diff. peak and hole [eÅ^{-3}]	2.599 and −0.990	1.936 and −2.710	0.804 and −0.563

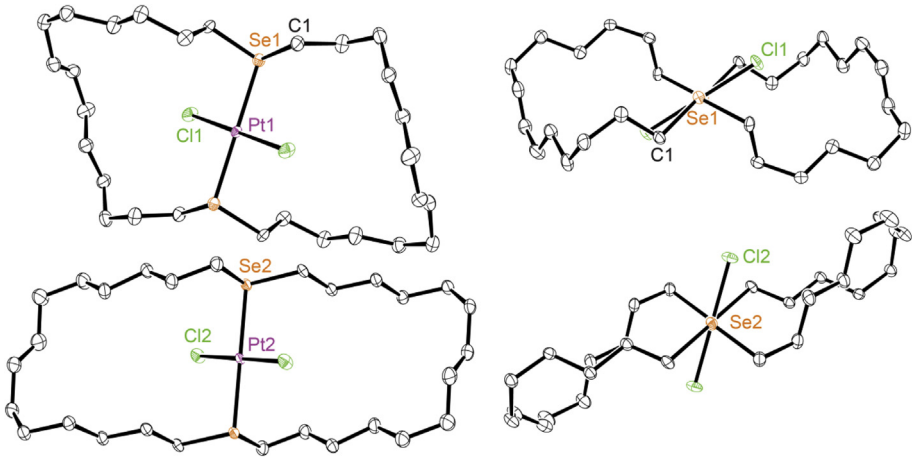

Fig. 1. Thermal ellipsoid plots (50% probability) of the two independent molecules of **11** in the unit cell. Views with the Se–Pt–Se axes in the plane of the paper (left) and perpendicular to the plane of the paper (right).

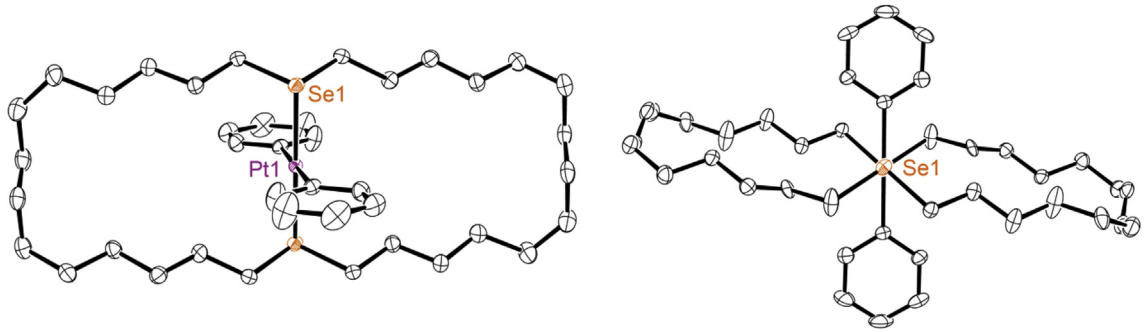

Fig. 2. Thermal ellipsoid plots (50% probability) of **12**. Views with the Se–Pt–Se axis in the plane of the paper (left) and perpendicular to the plane of the paper (right).

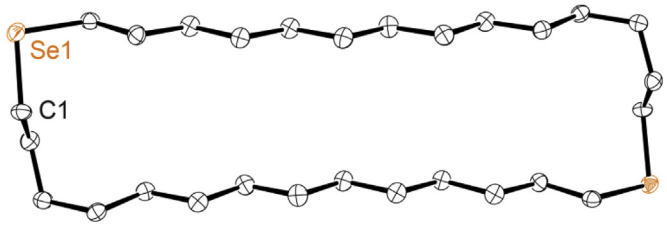

Fig. 3. Thermal ellipsoid plot (50% probability) of **13**. Key bond lengths [Å] and angles [°]: Se1–C1 1.968(3), Se1–C14 1.965(3), C1–Se1–C14 98.11(15).

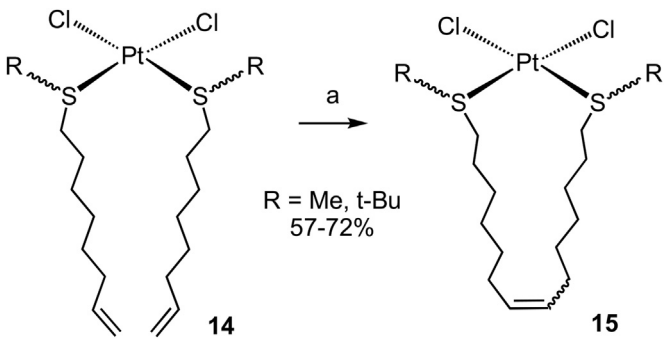

Scheme 4. Metatheses of related bis(dialkyl sulfide) complexes: (a) Grubbs' first generation catalyst, refluxing CH_2Cl_2.

bis(phosphine) complexes **6a-c** in Scheme 2, which lack a low energy equilibration pathway. For both series of compounds, the kinetic distribution will be governed as illustrated with **III** and **IV** in Scheme 5 (bottom). The first ring closing metathesis dictates the relative configurations of the heteroatom stereocenters, which in turn sets the *syn*/*anti* relationship of the heteroatom lone pairs or substituents.

Many types of chiral trivalent selenium compounds have been prepared, and the barriers to pyramidal inversion are usually quite high, e.g. on the order of 30–34 kcal/mol [17,18]. More extreme conditions are required as compared to analogous sulfur compounds. This is in part due to the higher p character of the orbitals used to make covalent bonds with selenium [19]. Accordingly, the C–Se–C bond angle in **13** (98.11(15)°) is closer to 90° than the ideal tetrahedral angle (109.5°). However, when one of the three substituents of a trivalent pyramidal heteroatom is a transition metal fragment, inversion barriers are significantly lowered [13,16,20]. This phenomenon is evident with **11**.

The intramolecular selenium-selenium distances in **11** and **12** range from 4.8486(8) to 4.7558(11) Å. These are slightly longer than the phosphorus-phosphorus distances in **2c**, *syn*-**6c**, and *anti*-**6c** (4.611, 4.621, and 4.588 Å, respectively). This variability is of interest from the standpoint of fine tuning barriers to Cl–Pt–Cl or PtX_2 rotation. For example, the rates of Fe(CO)(L)(L′) rotation are much faster in adducts of dibridgehead di*arsines* as opposed to dibridgehead diphosphines in **4a-c** (Scheme 1), due to the ca. 4% increase in the lengths of iron-arsenic vs. iron-phosphorus bonds [2b].

The diselenamacrocycle **13**, a thirty membered ring, is also of

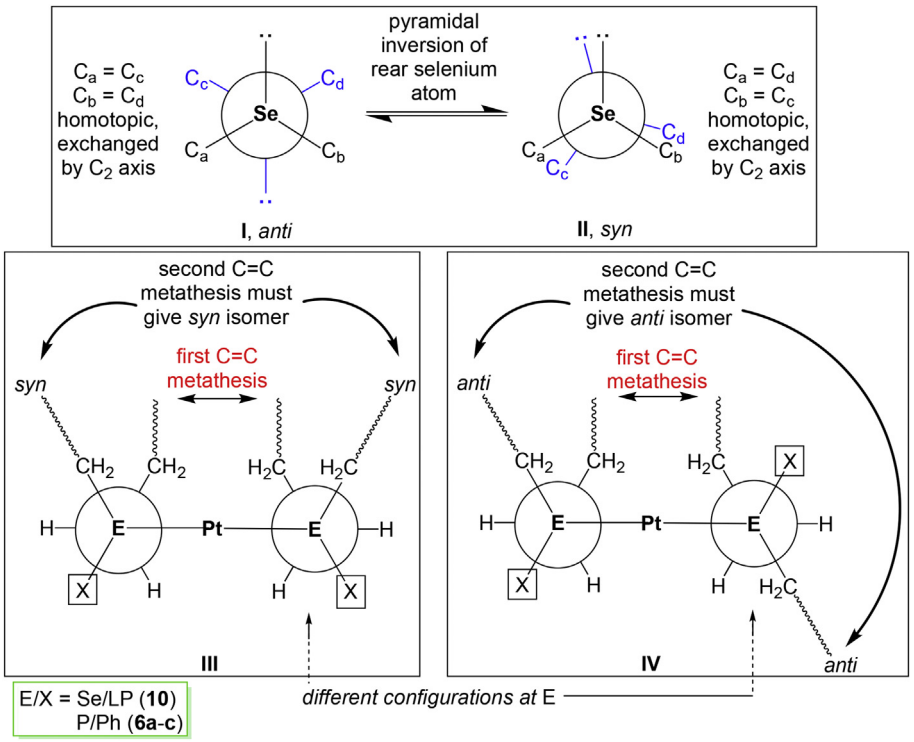

Scheme 5. Newman projections (Se–Pt–Se) representing *anti* (**I**) and *syn* (**II**) isomers of **11** and **12**, and mechanisms of formation of **11** and **6a-c**.

interest from several standpoints. It represents a rare type of saturated heterocycle, with the next largest system of formula $C_nH_{2n}Se_2$ featuring a fourteen membered ring [21] and the next largest a ten membered ring [22]. In the crystal, the selenium atoms are arrayed in an exodentate manner [23], and each initiates an extended $Se(CH_2)_9$ segment in which all torsion angles are ca. 180° (Fig. 3). This imparts a two dimensional rectangular shape, enabling the macrocycles to stack in columns in the lattice as depicted in Figure s2 (supporting information). The closest selenium-selenium contacts (4.93 Å, between columns) significantly exceed the sum of the van der Waals radii (1.90 + 1.90 Å) [24]. The structures of several unsaturated polyselenamacrocycles with C=C and C≡C linkages have been determined, and these also feature columnar packing motifs [25]. They exhibit similar or in some cases shorter (3.60–3.84 Å) selenium-selenium distances, the bonding implcations of which have been thoroughly analyzed [25].

In related work, it has proved possible to substitute the chloride ligands of **2c** and similar complexes by *p*-tolyl selenide (ArSe) ligands [14]. This raises the possibility of elaborating **11** to complexes with $PtSe_4$ coordination environments. There is currently much interest in molecular precursors to the binary phase $PtSe_2$, which sees use as a component in a variety of devices such as photodiodes and photovoltaic cells [26]. However, **11** or its chloride substitution products would not be very atom economical sources of platinum/selenium binary phases.

To our knowledge, there are no other types of *trans* spanning bis(selenium) donor ligands, but a dicationic platinum(II) adduct of a tetraselena crown ether links all *cis* and *trans* coordination sites [27]. A reviewer noted that a *cis* adduct of $PtCl_2$ and a 1,10-diselena analog of 18-crown-6 has also been reported [28]. Platinum(II) complexes of selenium donor ligands have received attention as anti-cancer agents [29], and selenoethers can also be effective in stabilizing metal nanoparticles [30].

In summary, this study has successfully extended the metathesis methodology in Schemes 1 and 2 to olefinic dialkyl selenide ligands, thereby providing the first doubly *trans*-spanning bis(-dialkyl selenide) complexes. However, subsequent hydrogenation steps are apparently inhibited, with forcing conditions leading to the concomitant release of diselenamacrocycles. Given the many unexpected findings above, additional types of complexes in which two methylene chains span *trans* donor atoms are now under investigation, and will be described in future reports.

4. Experimental section

4.1. General

Reactions (except hydrogenations) were conducted under inert atmospheres using standard Schlenk techniques. Chemicals were treated as follows: hexanes, CH_2Cl_2, toluene, and THF, dried and degassed using a Glass Contour solvent purification system; C_2H_5OH, $CHCl_3$, CH_3OH (EMD), benzene (BDH), $CDCl_3$ and CD_2Cl_2 (2 × Cambridge Isotope Laboratories), SiO_2 (Silicycle, 40–63 μm. 230–400 mesh), neutral Al_2O_3 (Macherey-Nagel), selenium powder (Alfa Aesar), $NaBH_4$ (Fisher Scientific), Na_2SO_4 (EMD), $PtCl_2$ (ABCR, 99.9%), Grubbs' catalyst $(Cy_3P)_2RuCl_2(=CHPh)$; Aldrich, 97%), Ph_2Zn (Acros, 95%), $(Ph_3P)_3RhCl$ (Lancaster, 97%), PtO_2 (Aldrich, 99.9%), and Pd/C (Alfa Aesar, 10%), used as purchased.

NMR spectra were recorded at ambient probe temperatures and referenced as follows (δ, ppm): ^1H, residual internal $CHCl_3$ (7.26), $CDHCl_2$ (5.32); $^{13}C\{^1H\}$, internal $CDCl_3$ (77.16), CD_2Cl_2 (53.5). Instruments used were identical to those specified in previous papers [3b].

$Se((CH_2)_6CH=CH_2)_2$ (9). A Schlenk flask was charged with selenium powder (0.798 g, 10.1 mmol) and C_2H_5OH (40 mL), and fitted with a condenser. The mixture was refluxed, and $NaBH_4$ (0.8134 g, 21.5 mmol) was added in portions until the black mixture turned colorless. A solution of $Br(CH_2)_6CH=CH_2$ (3.8031 g, 19.9 mmol) in C_2H_5OH (10 mL) was added with stirring. After 8 h (reflux), water (40 mL) and $CHCl_3$ (25 mL) were added. The organic

phase was separated, and the aqueous phase was extracted with $CHCl_3$ (3 × 25 mL). The combined organic phases were dried (Na_2SO_4). The solvent was removed by rotary evaporation to give **9** as a light yellow oil (2.720 g, 9.03 mmol, 91%). Anal. Calcd (%) for $C_{16}H_{30}Se$ (301.37): C, 63.77; H, 10.03; found C, 63.84; H, 9.94.

NMR ($CDCl_3$, δ/ppm): **^{1}H** (500 MHz) 5.76 (ddt, 2H, $^3J_{HHtrans}$ = 17.0 Hz, $^3J_{HHcis}$ = 10.3 Hz, $^3J_{HH}$ = 6.7 Hz, C*H*=), 4.96 (br d, 2H, $^3J_{HHtrans}$ = 17.0 Hz, =CH$_E$*H*$_Z$), 4.91 (br d, 2H, $^3J_{HHcis}$ = 10.8 Hz, =C*H*$_E$H$_Z$), 2.47–2.56 (m, 4H, C*H*$_2$), 2.04–2.00 (m, 4H, C*H*$_2$), 1.66–1.60 (m, 4H, C*H*$_2$), 1.39–1.28 (m, 12H, remaining C*H*$_2$); **^{13}C{^{1}H}** (126 MHz) 138.8 (s, *C*H=), 114.1 (s, =*C*H$_2$), 33.6 (s, *C*H$_2$CH=), 30.5 (s, *C*H$_2$), 29.7 (s, *C*H$_2$), 28.7 (s, *C*H$_2$), 28.5 (s, *C*H$_2$), 23.8 (s, *C*H$_2$). **IR** (cm^{-1}, powder film): 3075 (w), 2924 (s), 2855 (m), 1639 (w), 1458 (m), 994 (m), 910 (s), 726 (w).

***trans*-PtCl$_2$(Se((CH$_2$)$_6$CH=CH$_2$)$_2$)$_2$ (10).** A Schlenk flask was charged with **9** (1.205 g, 4.00 mmol), toluene (10 mL), and $PtCl_2$ (0.537 g, 2.02 mmol) with stirring. After 48 h, the mixture was concentrated to ca. 2 mL and placed at the top of a silica column (3.5 × 25 cm), which was eluted with hexanes/CH_2Cl_2 (70:30 to 50:50 v/v) and then CH_2Cl_2. The solvent was removed from the product containing fractions (assayed by tlc) by oil pump vacuum to give **10** as a yellow oil (1.471 g, 1.69 mmol, 85%). Anal. Calcd (%) for $C_{32}H_{60}Cl_2PtSe_2$ (868.73): C, 44.24; H, 6.96; found C, 44.46; H, 6.78.

NMR ($CDCl_3$, δ/ppm): **^{1}H** (500 MHz) 5.79 (ddt, 4H, $^3J_{HHtrans}$ = 17.0 Hz, $^3J_{HHcis}$ = 10.3 Hz, $^3J_{HH}$ = 6.7 Hz, C*H*=), 4.99 (br d, 4H, $^3J_{HHtrans}$ = 17.0 Hz, =CH$_E$*H*$_Z$), 4.93 (br d, 4H, 3J_{HHcis} = 10.8 Hz, =C*H*$_E$H$_Z$), 3.10–3.05 (m, 4H, C*H*$_2$), 2.70–2.64 (m, 4H, C*H*$_2$), 2.06–2.02 (m, 8H, C*H*$_2$), 1.87–1.81 (m, 8H, C*H*$_2$), 1.47–1.32 (m, 24H, remaining C*H*$_2$); **^{13}C{^{1}H}** (126 MHz) 138.4 (s, *C*H=), 114.2 (s, =*C*H$_2$), 33.6 (s, *C*H$_2$CH=), 30.8 (s, *C*H$_2$), 29.5 (s, *C*H$_2$), 28.6 (s, *C*H$_2$), 28.5 (s, *C*H$_2$), 28.2 (s, *C*H$_2$). **IR** (cm^{-1}, powder film): 3076 (w), 2924 (s), 2855 (m), 1637 (w), 1458 (m), 995 (m), 964 (m), 907 (s), 724 (m).

***trans*-PtCl$_2$(Se((CH$_2$)$_6$CH=CH(CH$_2$)$_6$)$_2$Se) (11).** A Schlenk flask was charged with **10** (1.746 g, 2.01 mmol), Grubbs' catalyst (0.0512 g, 0.0622 mmol, 3.1 mol%), and CH_2Cl_2 (750 mL; the resulting solution is 0.0027 M in **10**), and fitted with a condenser. The solution was refluxed with stirring (48 h), cooled, and passed through a pad of neutral alumina (10 cm). The solvent was removed from the filtrate by rotary evaporation. The residue was placed at the top of a silica column (3 × 24 cm), which was eluted with hexanes (500 mL) and then hexanes/CH_2Cl_2 (70:30 to 50:50 v/v). The solvent was removed from the product containing fractions (assayed by tlc) by rotary evaporation to give **11** as a light yellow solid (0.977 g, 1.12 mmol, 60%; mixture of isomers), mp (capillary) 116 °C, Anal. Calcd (%) for $C_{28}H_{52}Cl_2PtSe_2$ (816.65): C, 41.38; H, 6.45; found C, 42.09; H, 6.36 [31].

NMR (CD_2Cl_2, δ/ppm): **^{1}H** (500 MHz) 5.33 (m, 2H, C*H*=), 5.31 (m, 2H, C*H*=), 3.13 (m, 2H, C*H*$_2$), 3.06 (m, 2H, C*H*$_2$), 2.51–2.46 (m, 4H, C*H*$_2$), 2.01 (m, 8H, C*H*$_2$), 1.90 (m, 8H, C*H*$_2$), 1.51–1.27 (m, 24H, remaining C*H*$_2$); **^{13}C{^{1}H}** (126 MHz) (major isomer only) 131.6 (s, *C*H=), 32.7 (s, *C*H$_2$CH=), 32.3 (s, *C*H$_2$), 30.2 (s, *C*H$_2$), 29.6 (s, *C*H$_2$), 29.2 (s, *C*H$_2$), 28.7 (s, *C*H$_2$). **IR** (cm^{-1}, powder film): 2924 (s), 2846 (m), 1445 (m), 964 (m), 723 (m).

***trans*-PtPh$_2$(Se((CH$_2$)$_6$CH=CH(CH$_2$)$_6$)$_2$Se) (12).** A Schlenk flask was charged with **11** (0.163 g, 0.199 mmol), Ph_2Zn (0.132 g, 0.600 mmol), and THF (10 mL) with stirring. After 20 h, CH_3OH (several drops) were added and the sample was exposed to air. After 1 h, the solvent was removed by rotary evaporation, and benzene (5.0 mL) was added. The suspension was filtered through a pipette filled with silica, which was rinsed with benzene. The solvent was removed from the combined filtrate by rotary evaporation to give **12** as a white powder (0.1534 g, 0.171 mmol, 86%; mixture of isomers), mp (capillary) 140 °C, Anal. Calcd (%) for $C_{40}H_{62}PtSe_2$ (895.92): C, 53.62; H, 6.98; found C, 53.80; H, 6.89.

NMR ($CDCl_3$, δ/ppm) [32]: **^{1}H** (500 MHz) 7.39 (m, 4H, *o*-Ph), 7.07 (m, 4H, *m*-Ph), 6.86 (m, 2H, *p*-Ph), 5.47 (m, 2H, =CH), 5.44 (m, 2H, =CH), 2.59–2.54 (m, 2H, C*H*$_2$), 2.47–2.42 (m, 2H, C*H*$_2$), 2.28–1.77 (br m, 20H, C*H*$_2$), 1.44–1.39 (m, 24H, remaining C*H*$_2$); **^{13}C{^{1}H}** (126 MHz) (major isomer only) 163.3 (s, *i*-Ph), 139.4 (s, *o*-Ph), 131.2 (s, *C*H=), 127.2 (s, *m*-Ph), 121.7 (s, *p*-Ph), 32.2 (s, *C*H$_2$CH=), 30.8 (s, *C*H$_2$), 29.8 (s, *C*H$_2$), 29.4 (s, *C*H$_2$), 28.8 (s, *C*H$_2$), 28.1 (s, *C*H$_2$). **IR** (cm^{-1}, powder film): 3040 (w), 2984 (m), 2915 (s), 2846 (m), 1560 (w), 1425 (m), 964 (m), 703 (s).

4.2. Hydrogenations

A Fischer-Porter bottle was charged with **11** (0.8133 g, 0.996 mmol), CH_2Cl_2 (15 mL), PtO_2 (0.0454 g, 0.200 mmol), and H_2 (5 bar). The mixture was kept at 50 °C (venting H_2 to maintain 5 bar) and stirred (96 h). The solvent was removed by rotary evaporation. The residue was filtered through a short pad of silica (3 × 10 cm, rinsed with CH_2Cl_2). The solvent was removed from the combined filtrate by rotary evaporation to give unreacted **11** as a light yellow solid, as assayed by ^{1}H and ^{13}C NMR. **B.** Procedure A was repeated, but with $(Ph_3P)_3RhCl$ in place of PtO_2. The result was identical. **C.** A Fischer-Porter bottle was charged with **11** (0.813 g, 0.996 mmol), C_2H_5OH (15 mL), 10% Pd/C (0.0532 g, 0.500 mmol), and H_2 (8 bar). The mixture was kept at 85 °C (venting H_2 to maintain 8 bar) and stirred (96 h). The mixture was filtered through a short pad of silica (3 × 10 cm, rinsed with CH_2Cl_2). The solvent was removed from the combined filtrate by rotary evaporation. Hexane (10 mL) was added. The solid was collected by filtration and dried by oil pump vacuum to give Se($C_{14}H_{28}$)$_2$Se (**13**) as a white solid (0.3972 g, 0.721 mmol, 72%), mp (capillary) 59–61 °C, Anal. Calcd (%) for $C_{28}H_{56}Se_2$ (550.66): C, 61.07; H, 10.25; found C, 60.91; H, 10.47. **D.** Procedure C was repeated, but with **12** (0.790 g, 0.881 mmol), C_2H_5OH (15 mL), 10% Pd/C (0.0507 g, 0.476 mmol), and H_2 (8 bar). An identical workup gave **13** as a white solid (0.325 g, 0.590 mmol, 67%).

NMR ($CDCl_3$, δ/ppm): **^{1}H** (500 MHz) 2.55 (t, 8H, ^3J = 6.8 Hz, C*H*$_2$), 1.69–1.63 (m, 8H, C*H*$_2$), 1.41–1.36 (m, 8H, C*H*$_2$), 1.27 (br s, 32H, remaining C*H*$_2$); **^{13}C{^{1}H}** (126 MHz) 30.6 (s, *C*H$_2$), 29.7 (s, *C*H$_2$), 29.4 (s, *C*H$_2$), 29.3 (s, *C*H$_2$), 29.2 (s, *C*H$_2$), 28.8 (s, *C*H$_2$), 23.8 (s, *C*H$_2$). **IR** (cm^{-1}, powder film): 2915 (s), 2850 (m), 1462 (m), 1354 (m), 1279 (s), 1123 (m), 715 (m).

4.3. Crystallography

A. A CH_2Cl_2/hexane solution of **11** (4 mL, 3:1 v/v) was allowed to slowly concentrate. After 5 d, yellow plates were collected and data obtained as outlined in Table 1. Cell parameters were obtained from 45 frames using a 1° scan and refined with 44553 reflections. Integrated intensity information for each reflection was obtained by reduction of the data frames with the program APEX3 [33]. Lorentz and polarization corrections were applied. Data were scaled, and adsorption corrections were applied using the program SADABS [34]. The space group was determined from systematic reflection conditions and statistical tests. The structure was refined (weighted least squares refinement on F^2) to convergence [35,36]. Olex2 [36] was employed for the final data presentation and structure plots. Non-hydrogen atoms were refined with anisotropic thermal parameters. Hydrogen atoms were fixed in idealized positions using a riding model. The absence of additional symmetry or voids was confirmed using PLATON (ADDSYM) [37]. The unit cell contained two independent molecules, each with crystallographic inversion center. **B.** A CH_2Cl_2 solution of **12** was allowed to slowly concentrate. After 2 d, colorless blocks were collected and data obtained as outlined in Table 1. The structure was solved as in A (60 frames, 48342 reflections). Two segments of one methylene chain were disordered, but could be successfully modeled between two

positions (C11–C15, C18–C20; 50:50 occupancy). The molecule featured a crystallographic inversion center. **C.** A hexane/CH_2Cl_2 solution of **13** (4 mL, 3:1 v/v) was allowed to slowly concentrate. After 3 d, colorless plates were collected and data obtained as outlined in Table 1. The structure was solved as in A (45 frames, 17649 reflections), and featured a crystallographic inversion center.

Notes

The authors declare no competing financial interest.

Acknowledgement

The authors thank the US National Science Foundation (CHE-1566601) for support and Prof. Igor Alabugin (Florida State University) for helpful comments.

Appendix A. Supplementary data

Supplementary data to this article can be found online at https://doi.org/10.1016/j.jorganchem.2018.08.029.

References

[1] S.H.A.M. Leenders, R. Gramage-Doria, B. de Bruin, J.N.H. Reek, Transition metal catalysis in confined spaces, Chem. Soc. Rev. 44 (2015) 433–448.

[2] Prototype studies involving $Fe(CO)_3$ adducts. a) G.M. Lang, T. Shima, L. Wang, K.J. Cluff, F. Hampel, J. Blümel, J.A. Gladysz, Gyroscope-like complexes based on dibridgehead diphosphine cages that are accessed by three-fold intramolecular ring closing metatheses and encase $Fe(CO)_3$, $Fe(CO)_2(NO)^+$, and $Fe(CO)_3(H)^+$ rotators, J. Am. Chem. Soc. 138 (2016) 7649–7663;
b) G.M. Lang, N. Bhuvanesh, J.H. Reibenspies, J.A. Gladysz, Syntheses, reactivity, structures, and dynamic properties of gyroscope-like iron carbonyl complexes based on dibridgehead diarsine cages, Organometallics 35 (2016) 2873–2889;
c) G.M. Lang, D. Skaper, F. Hampel, J.A. Gladysz, Synthesis, reactivity, structures, and dynamic properties of gyroscope like iron complexes with dibridgehead diphosphine cages: pre- *vs.* post-metathesis substitutions as routes to adducts with neutral dipolar Fe(CO)(NO)(X) rotors, Dalton Trans. 45 (2016) 16190–16204.

[3] Prototype studies involving MCl_2 adducts. a) A.J. Nawara-Hultzsch, M. Stollenz, M. Barbasiewicz, S. Szafert, T. Lis, F. Hampel, N. Bhuvanesh, J.A. Gladysz, Gyroscope-like molecules consisting of PdX_2/PtX_2 rotators within three-spoke dibridgehead diphosphine stators: syntheses, substitution reactions, structures, and dynamic properties, Chem. Eur J. 20 (2014) 4617–4637;
b) S. Kharel, H. Joshi, N. Bhuvanesh, J.A. Gladysz, Syntheses, structures, and thermal properties of gyroscope like complexes consisting of $PtCl_2$ rotators encased in macrocyclic dibridgehead diphosphines $P((CH_2)_n)_3P$ with extended methylene chains (n = 20/22/30), and isomers thereof, Organometallics 37 (2018) 2991–3000.

[4] Prototype studies involving $M(CO)_x(X)_{4-x}$ adducts (x = 2, 3). a) T. Fiedler, N. Bhuvanesh, F. Hampel, J.H. Reibenspies, J.A. Gladysz, Gyroscope like molecules consisting of trigonal or square planar osmium rotators within three-spoked dibridgehead diphosphine stators: syntheses, substitution reactions, structures, and dynamic properties, Dalton Trans. 45 (2016) 7131–7147;
b) G.D. Hess, T. Fiedler, F. Hampel, J.A. Gladysz, Octahedral gyroscope-like molecules consisting of rhenium rotators within cage-like dibridgehead diphosphine stators: syntheses, substitution reactions, structures, and dynamic properties, Inorg. Chem. 56 (2017) 7454–7469.

[5] See also L. Wang, F. Hampel, J.A. Gladysz, "Giant" gyroscope-like molecules consisting of dipolar Cl-Rh-CO rotators encased in three-spoke stators that define 25–27-membered macrocycles, Angew. Chem. Int. Ed. 45 (2006) 4372–4375. "Gyroskop-Giganten": dipolare Cl-Rh-CO-Rotatoren, umgeben von Statoren aus drei Speichen 25- bis 27-gliedriger Makrocyclen, Angew. Chem. 118 (2006) 4479-4482.

[6] a) G.S. Kottas, L.I. Clarke, D. Horinek, J. Michl, Artificial molecular rotors, Chem. Rev. 105 (2005) 1281–1376;
b) P. Commins, M.S. Garcia-Garibay, Photochromic molecular gyroscope with solid state rotational states determined by an azobenzene bridge, J. Org. Chem. 79 (2014) 1611–1619 (and earlier work by this group cited therein).

[7] T. Shima, E.B. Bauer, F. Hampel, J.A. Gladysz, Alkene metatheses in transition metal coordination spheres: dimacrocyclizations that join *trans* positions of square-planar platinum complexes to give topologically novel diphosphine ligands, Dalton Trans. 33 (2004) 1012–1018.

[8] E. Steigleder, T. Shima, G.M. Lang, A. Ehnbom, F. Hampel, J.A. Gladysz, Partially shielded $Fe(CO)_3$ rotors: syntheses, structures, and dynamic properties of complexes with doubly trans spanning diphosphines, *trans*-$Fe(CO)_3(PhP((CH_2)_n)_2PPh)$, Organometallics 36 (2017) 2891–2901.

[9] Related square planar complexes with doubly bridged trans nitrogen donor atoms: P.D. Zeits, G.P. Rachiero, F. Hampel, J.H. Reibenspies, J.A. Gladysz, Gyroscope-like platinum and palladium complexes with trans-spanning bis(-pyridine) ligands, Organometallics 31 (2012) 2854–2877.

[10] Functionalization of the sulfur lone pair in dialkyl sulfide complexes a) W.A. Schenk, J. Frisch, M. Dürr, N. Burzlaff, D. Stalke, R. Fleischer, W. Adam, F. Prechtl, A. Smerz, Oxidation of thioether ligands in pseudotetrahedral cyclopentadienylruthenium complexes: toward a new stereoselective synthesis of chiral sulfoxides, Inorg. Chem. 36 (1997) 2372–2378 (and earlier work by this group cited therein);
b) M. Otto, B.J. Boone, A.M. Arif, J.A. Gladysz, Synthesis, structure, and interconversion of chiral rhenium oxygen- and sulfur-bound sulfoxide complexes of formula $[(\eta^5\text{-}C_5H_5)Re(NO)(PPh_3)(OS(Me)R)]^+ X^-$; diastereoselective oxidations of coordinated methyl alkyl sulfides, J. Chem. Soc., Dalton Trans. 30 (2001) 1218–1229, see for example Scheme 4 therein.

[11] a) D.L. Klayman, T.S. Griffin, Reaction of selenium with sodium borohydride in protic solvents. A facile method for the introduction of selenium into organic molecules, J. Am. Chem. Soc. 95 (1973) 197–199;
b) O. Prakash, K.N. Sharma, H. Joshi, P.L. Gupta, A.K. Singh, Half sandwich complexes of chalcogenated pyridine based bi-(N, S/Se) and terdentate (N, S/Se, N) ligands with (η^6-benzene)ruthenium(II): synthesis, structure and catalysis of transfer hydrogenation of ketones and oxidation of alcohols, Dalton Trans. 42 (2013) 8736–8747 (and earlier work by this group cited therein);
c) A.R.M. de Oliveira, L. Piovan, F. Simonelli, A. Barison, M. de Fatima, C. Santos, M.B.M. de Mello, A ^{77}Se NMR study of elemental selenium reduction using $NaBH_4$, J. Organomet. Chem. 806 (2016) 54–59.

[12] a) A.J. Nawara-Hultzsch, K. Skopek, T. Shima, M. Barbasiewicz, G.D. Hess, D. Skaper, J.A. Gladysz, Syntheses and palladium, platinum, and borane adducts of symmetrical trialkylphosphines with three terminal vinyl groups, $P((CH_2)_mCH{=}CH_2)_3$, Z. Naturforsch. 65b (2010) 414–424;
b) M. Stollenz, H. Joshi, S. Kharel, T. Fiedler, N. Bhuvanesh, J.A. Gladysz, Platinum complexes containing or derived from olefinic phosphines $P(X)((CH_2)_6CH{=}CH_2)_2$ (X = OH, Ph, $(CH_2)_6CH{=}CH_2$); ring closing metatheses, structures, and *trans/cis* isomerizations, Polyhedron, (in press), https://doi.org/10.1016/j.poly.2018.09.025.

[13] R.J. Cross, T.H. Green, R. Keat, Inversion of configurations at pyramidal sulphur, selenium, and tellurium in diethyl chalcogen complexes of platinum(II) and palladium(II), J. Chem. Soc., Dalton Trans. (1976) 1150–1152.

[14] D. Taher, A.J. Nawara-Hultzsch, N. Bhuvanesh, F. Hampel, J.A. Gladysz, Mono- and disubstitution reactions of gyroscope like complexes derived from Cl-Pt-Cl rotators within cage like dibridgehead diphosphine ligands, J. Organomet. Chem. 821 (2016) 136–141.

[15] J. Ruwwe, J.M. Martín-Alvarez, C.R. Horn, E.B. Bauer, S. Szafert, T. Lis, F. Hampel, P.C. Cagle, J.A. Gladysz, Olefin metatheses in metal coordination spheres: versatile new strategies for the construction of novel monohapto or polyhapto cyclic, macrocyclic, polymacrocyclic, and bridging ligands, Chem. Eur. J. 7 (2001) 3931–3950.

[16] N. Quirós Méndez, A.M. Arif, J.A. Gladysz, Synthesis, structure, and dynamic behavior of rhenium sulfide and sulfoxide complexes of the formula $[(\eta^5\text{-}C_5H_5)Re(NO)(L)(XRR')]^+ X'^-$ (X = S, SO), Organometallics 10 (1991) 2199–2209 (see Scheme 5 therein).

[17] Studies where inversion barriers for organic compounds with trivalent selenium stereocenters have been reported. a) N. Kamigata, Y. Nakamura, K. Kikuchi, I. Ikemoto, T. Shimizu, H.J. Matsuyama, Synthesis and stereochemistry of an optically active selenonium ylide. X-Ray molecular structure of $(+)_{Se}$-{4′-[(−)-menthyloxycarbonyl]phenyl}(methyl)-selenonium 4,4-dimethyl-2,6-dioxocyclohexylide, J. Chem. Soc. Perkin Trans. 1 (1992) 1721–1727;
b) N. Kamigata, H. Taka, A. Matsuhisa, T.J. Shimizu, Kinetic studies on the pyramidal inversion of optically active selenonium imides, J. Phys. Org. Chem. 8 (1995) 139–142;
c) H. Taka, S. Shimizu, F. Iwasaki, M. Yasui, N. Kamigata, Isolation and stereochemistry of optically active selenonium imides, J. Org. Chem. 64 (1999) 7433–7438;
d) A. Wiegrefe, T. Brinkmann, H.C. Uzar, Effect of solvent on the inversion of pyramidal sulfonium and selenonium compounds, J. Phys. Org. Chem. 14 (2001) 205–209.

[18] T. Shimizu, N. Kamigata, S. Ikuta, Pyramidal inversion energies and conformational analysis of chalcogen-onium imides based on ab initio MO calculations, J. Chem. Soc., Perkin 2 (1999) 1469–1473.

[19] I.V. Alabugin, Stereoelectronic Effects: a Bridge between Structure and Reactivity, John Wiley & Sons, Hoboken, New Jersey, 2016, pp. 71–73 (see "Sulfur").

[20] Additional examples with platinum(II): D.K. Wicht, I. Kovacik, D.S. Glueck, Chiral terminal platinum(II) phosphido complexes: synthesis, phosphorus inversion, and acrylonitrile insertion, Organometallics 18 (1999) 5141–5151.

[21] H. Higuchi, K. Tani, T. Otsubo, Y. Sakata, S. Misumi, New synthetic method of [2.2]cyclophanes via diselena[3.3]cyclophanes, Bull. Chem. Soc. Jpn. 60 (1987) 4027–4036 (see compound 31 therein).

[22] a) J.S.L. Yeo, J.J. Vittal, T.S.A. Hor, Facile metal-mediated synthesis of macrocyclic diselenoethers, Eur. J. Inorg. Chem. (2003) 277–280;
b) H. Fujihara, R. Akaishi, N. Furukawa, Preparation and reactivity of

dichalcogenide (S, Se) dication salts from medium-sized cyclic bis-sulfide and bis-selenides, Tetrahedron 49 (1993) 1605–1618.
[23] a) B. de Groot, S.J. Loeb, Crown thioether ligands containing rigid xylyl units. Synthesis and structure of 2,5,8,-trithia[9]-*o*-benzenophane (TTOB), 2,5,8-trithia[9]-*m*-benzenophane (TTMB), and *fac*-$Mo(CO)_3$(TTOB)·DMSO, Inorg. Chem. 29 (1990) 4084–4090;
b) B. de Groot, H.A. Jenkins, S.J. Loeb, Exodentate versus endodentate coordination of a crown thioether ligand in silver(I) complexes of 2,5,8-trithia[9]-*o*-benzenophane (TT[9]OB). Structures of $[Ag(TT[9]OB)_2][X]$ (X = ClO_4, BPh_4, CF_3SO_3), Inorg. Chem. 31 (1992) 203–208.
[24] A. Bondi, van der Waals volumes and radii, J. Phys. Chem. 68 (1964) 441–451.
[25] a) D.B. Werz, T.H. Staeb, C. Benisch, B.J. Rausch, F. Rominger, R. Gleiter, Self-organization of chalcogen-containing cyclic alkynes and alkenes to yield columnar structures, Org. Lett. 3 (2002) 339–342;
b) D.B. Werz, R. Gleiter, F.J. Rominger, Cyclic tetra- and hexaynes containing 1,4-donor-substituted butadiyne units: synthesis and supramolecular organization, J. Org. Chem. 69 (2004) 2945–2952.
[26] a) K. Ullah, S. Ye, Z. Lei, K.-Y. Cho, W.-C. Oh, Synergistic effect of $PtSe_2$ and graphene sheets supported by TiO_2 as cocatalysts synthesized via microwave techniques for improved photocatalytic activity, Catal. Sci. Technol. 5 (2015) 184–198;
b) C. Yim, K. Lee, N. McEvoy, M. O'Brian, S. Riazimehr, N.C. Berner, C.P. Cullen, J. Kotakoski, J.C. Meyer, M.C. Lemme, G.S. Duesberg, High-performance hybrid electronic devices from layered $PtSe_2$ films grown at low temperature, ACS Nano 10 (2016) 9550–9558;
c) C. Yim, N. McEvoy, S. Riazimehr, D.S. Schneider, F. Gity, S. Monaghan, P.K. Hurley, M.C. Lemme, G.S. Duesberg, Wide spectral photoresponse of layered platinum diselenide-based photodiodes, Nano Lett. 18 (2018) 1794–1800.
[27] N.R. Champness, P.F. Kelly, W. Levason, G. Reid, A.M.Z. Slawin, D.J. Williams, Selenoether macrocyclic chemistry: syntheses, NMR studies, redox properties, and single-crystal structures of $[M([16]aneSe_4)](PF_6)_2$·2MeCN (M = Pd, Pt; [16]aneSe_4 = 1,5,9,13-tetraselenacyclohexadecane), Inorg. Chem. 34 (1995) 651–657.
[28] M.J. Hesford, W. Levason, M.L. Matthews, G. Reid, Synthesis and complexation of the mixed tellurium-oxygen macrocycles 1-tellura-4,7-dioxacyclononane, [9]aneO_2Te, and 1,10-detellura-4,7,13,16-tetraoxacyclooctadecane, [18]aneO_4Te_2 and their selenium analogues, Dalton Trans. (2003) 2852–2858.
[29] F. Li, T. Li, X. Han, H. Zhuang, G. Nie, H. Xu, Nanomedicine assembled by co-ordinated selenium-platinum complexes can selectively induce cytotoxicity in cancer cells by targeting the glutathione antioxidant defense system, ACS Biomater. Sci. Eng. 4 (2018) 1954–1962 (and earlier studies by this group cited therein).
[30] G.K. Rao, A. Kumar, B. Kumar, A.K. Singh, Didocosyl selenide stabilized recyclable Pd(0) nanoparticles and coordinated palladium(II) as efficient catalysts for Suzuki–Miyaura coupling, Dalton Trans. 41 (2012) 4306–4309.
[31] This microanalysis is only in marginal agreement with the empirical formula, but is nonetheless reported as the best obtained to date. F.P. Gabbaï, P.J. Chirik, D.E. Fogg, K. Meyer, D.J. Mindiola, L.L. Schafer, S.-L. You, An editorial about elemental analysis, Organometallics vol. 35 (2016) 3255–3256.
[32] The ortho, meta, and para ^1H and ^{13}C NMR signals were assigned by analogy to those of similar compounds reported earlier [3a,14].
[33] APEX3, Bruker AXS Inc., Madison, WI, USA, 2012.
[34] G.M. Sheldrick, SADABS, Bruker AXS Inc., Madison, WI, USA, 2001.
[35] a) G.M. Sheldrick, A short history of SHELX, Acta Crystallogr. A64 (2008) 112–122;
b) G.M. Sheldrick, SHELXT - integrated space-group and crystal-structure determination, Acta Crystallogr. A71 (2015) 3–8;
c) G.M. Sheldrick, Crystal structure refinement with SHELXL, Acta Crystallogr. C71 (2015) 3–8.
[36] O.V. Dolomanov, L.J. Bourhis, R.J. Gildea, J.A.K. Howard, H. Puschmann, OLEX2: a complete structure solution, refinement and analysis program, J. Appl. Crystallogr. 42 (2009) 339–341.
[37] A.L. Spek, Single-crystal structure validation with the program PLATON, J. Appl. Crystallogr. 36 (2003) 7–13.